DE GRUYTER OPEN

Journal of MECHANICAL ENGINEERING – Strojnícky časopis,
VOL 67 (2017), NO 1, 77 - 86

STU SjF

MECHANICAL AND WEAR PROPERTIES OF FRICTION STIR WELDED 0-6WT% nAl_2O_3 REINFORCED Al-13WT%Si COMPOSITES

PATEL Vinay Kumar[1], RANI Komal[1]

[1]Govind Ballabh Pant Engineering College Ghurdauri, Department of Mechanical Engineering, Pauri Garhwal 246001, Uttarakhand, India, email: vinaykrpatel@gmail.com

Abstract: Friction Stir Welding (FSW) of an Al-13%Si alloy matrix reinforced with 0, 3 and 6 wt% Al_2O_3 nanoparticles (nAl_2O_3) is performed and the optical microstructures, tensile strength, hardness and sliding wear properties of friction stir welded joints are investigated and compared to those of base materials. Four different zones of distinct appearances were observed during FSW, which exhibited altered microstructures in the nugget zone (NZ), thermo mechanically affected zone (TMAZ), heat affected zone (HAZ), and base material zone (BMZ). The ultimate tensile strength of the base materials and their welded joints were found to be increasing with increased wt% of nano-alumina reinforcements. High joint efficiency of 89-97% was achieved in FSW. Hardness and wear resistance of friction stir welded joints were found to be better than those of the base materials.

KEYWORDS: Friction stir welding, Metal matrix composite, Mechanical properties, Al-Si alloy, Alumina, Wear

1 Introduction

Various hard micro/nanoscale ceramic particle reinforced aluminium matrix composites are among the most widely studied metal matrix composite materials owing to their excellent material properties such as high specific strength and stiffness, low density, low thermal expansion and enhanced creep and wear resistance. The widespread usage of these metal matrix composites with the advancements of various ceramic particles is severely limited due to inadequate and inefficient secondary processing or manufacturing techniques such as machining and welding. The Welding Institute (TWI) UK [1] patented a solid-state joining method "friction stir welding" which has been used widely to produce high quality welds in many materials like aluminium, nickel, magnesium, titanium and steel for applications in automobiles [2], shipbuilding [2], high-speed train manufacturing [2, 3] and aviation industry [2, 4]. Friction stir welding has also gained recognition as an efficient method for joining various aluminium metal matrix composites reinforced with Al_2O_3 [5], SiC [6-7], B_4C [8], TiB_2 [9], Mg_2Si [10], TiC [11], and ZrB_2 [12].

Friction stir welding has an advantage over fusion welding of metal matrix composites owing to the absence of any kind of segregation and/or reaction to the reinforcements, hot cracking and porosity during the solid phase welding process. Al-Si alloy is one of the most popular materials for aerospace, automobile, and marine industries due to its high fluidity and castability, low density, high specific strength and good corrosion properties [13, 14]. Silicon is known for reducing thermal expansion and increasing wear and corrosion resistance of the alloy [15]. Ceramic reinforcements further improve the wear resistance properties of Al-Si alloys. Absence of melting in FSW diminishes the probability of defect formation and recovers the mechanical properties which enable FSW a capable joining method for metal matrix composites (MMCs). Several studies have been performed on FSW of micro-sized alumina

DOI: 10.1515/scjme-2017-0008, Print ISSN 0039-2472, On-line ISSN 2450-5471

reinforced aluminium MMCs but only a few articles [16] have been dedicated to FSW of aluminium with silicon matrix composite. Moreover, it seems that there has been no investigation carried out on the FSW of MMCs such as Al-13%Si reinforced with nanoscale alumina. Current research is focused on FSW of Al-13%Si alloy matrix reinforced with nAl_2O_3 particles and comparative investigations of the microstructures, tensile, hardness and wear properties of parent composites and their welded joints.

2 Experimental details

2.1 Composite fabrication

Three different kinds of composites were prepared by stir casting method in the present work utilizing Al-13%Si as the matrix material and varying reinforcements of alumina nanoparticles (weight percentage 0, 3 and 6 % respectively). Ex-situ fabrication technique was employed for fabrication of these composites. The nano-alumina powders had the following physical properties: density - 3.69 g/cm^3, average particle size - 40 nm and elastic modulus - 300 GPa. Magnesium (1.5 wt%) was added for improved wettability between reinforcement and the matrix. Initially, aluminium with 13% silicon alloy is melted in a muffle furnace with 1.0 wt% zinc chloride added as flux material for removal of impurities. Reinforcing nano-alumina particles preheated in the muffle furnace at 400-500 ^oC were introduced into the molten material at a rate of 0.5 g/sec. Stirring was performed at a rate of 250-300 rpm when adding reinforcements. Stirring was continued for 4-5 minute after pouring of whole particles. By the end, molten material was poured into a metallic mould which was prefixed inside silica sand. Each Plate, with a dimension of 100×55×6 mm^3, was prepared with the help of a hacksaw and vertical milling machine.

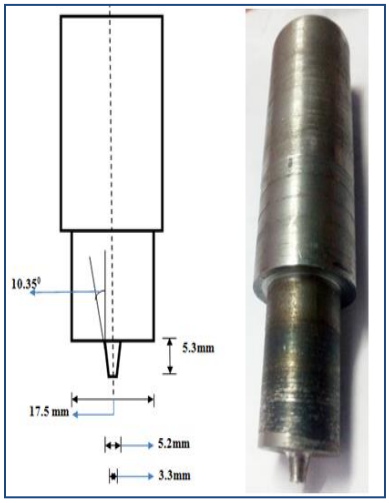

Fig. 1 FSW tool as prepared (right) to the required dimension (left)

2.2 Fabrication of tool

The tool consisted of two main parts designated as the shoulder and pin. The pin profile of the tapered section and the flat shoulder of the mild steel tool were prepared by a turning operation on a lathe machine to execute the FSW process. The parameters of the prepared tool are displayed in Fig. 1.Optimum parameters were decided on the basis on experiments with least joints' defects. The tool traverse and rotational speed of 20 mm/min and 2000 rpm respectively was selected and proved satisfactory for defect free FSW of all three types of the composites. A BF-5U vertical milling machine (Batliboi make) was employed for execution of the FSW process. A plate fixing arrangement shown in Fig. 2 was prepared for fixing the plates

with sufficient rigidity. Mild steel backing plates were used as supports from the bottom side. The setup was fixed with the help of a nut and bolt during welding.

Fig. 2 Set-up for FSW

2.3 Preparation of test and microscopy samples

Various mechanical tests were performed on friction welded joints to estimate the suitability and applicability of these joints for various service conditions [17]. The samples for tensile tests were prepared according to ASTM E-08 standard as shown in Fig. 3 along the transverse direction of the joint. Tensile tests were performed on computerized Universal Testing Machine HEICO-HL590 with a cross-head speed of 10 mm/min. Hardness test was carried out over the cross-section of different zones. Brinell hardness testing machine with 62.5 kg applied load was employed for hardness measurements taken in the present work.

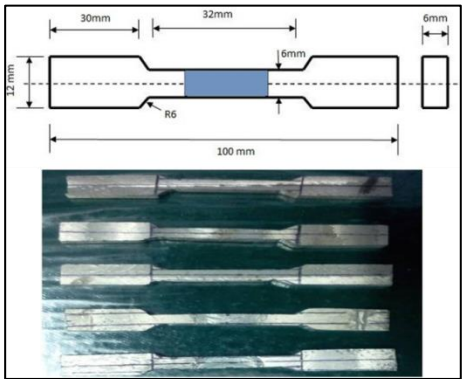

Fig. 3 Tensile test samples of required dimension as per ASTM E-08

Sliding wear behaviour of composite materials was measured on Ducom sliding wear test rig ED-201. Samples for dry sliding wear were prepared for the weld zone according to ASTM G99-04 as shown in Fig. 4. Normal loads of 2, 2.5 and 3 kg were applied to the samples of each composition for a duration of 30 min.

Fig. 4 Sliding wear test samples

A BANBROS made metallurgical microscope (BMI-101A) with digital camera connected to a computer was used for optical observation of the microstructures. Microstructural study was conducted on cross-section of friction stir welded plate. For microstructural observation, the surface was prepared by first grinding with emery paper at 120, 240, 320, 400 grit sizes followed by fine grit paper of sizes 0, 2, 3, 4. The direction of sample rubbing was changed to 90^o each time the paper size was changed. Finally the samples were polished on a single disc polishing machine (Hifin diamond compound hifinator) for 30 minutes. The Poultan etchant (2ml HF, 3ml HCL, 20ml HNO_3 and 175ml water) was employed for observing the grains' distribution.

3 Results and discussion

FSW joints exhibited semi-circular rings where the tool shoulder had continuous contact with the upper surface with the plates. The opposite side of the plates showed only a single line as a mark of joint. These semi-circular rings on the upper surface represented the material flow pattern of plastically deformed material during FSW.

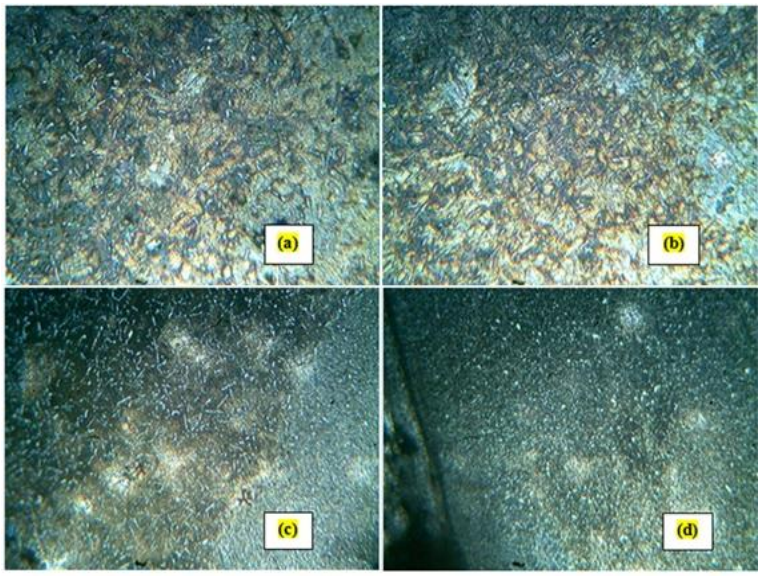

Fig. 5 Microstructure of Al-13%Si Alloy (a) Base Material, (b) Heat Affected Zone, (c) Transition Zone and (d) Nugget Zone

3.1 Microstructures

The Microstructure observations performed by optical microscopy of pure Al-13%Si alloy and their composites with 3 and 6% nano-alumina are shown in Fig. 5, Fig. 6 and Fig. 7 respectively. Low magnification optical image of these joints confirmed the formation of four different zones owing to their different appearances. These four zones were designated as the nugget zone (NZ), thermo mechanically affected zone (TMAZ), heat affected zone (HAZ), and base material zone (BMZ). FSW affected each zone differently, so each zone had distinct microstructure. The nugget zone suffered excessive plastic deformation and dynamic recrystallization due to the tool stirring action. Homogeneous distribution of reinforcements and fine grains of matrix were observed in the NZ due to the tool action. TMAZ were also thermally and mechanically affected by the tool stirring action. Heat produced during FSW had severe effects on the TMAZ micro-structure. The FSW tool rotated the matrix grains up to 90^o along the TMAZ. The HAZ exhibited coarse grains as compared to BMZ. The role of heat generation during FSW and the corresponding temperature distribution in the aluminium alloy has also been suggested to play a major role in the modification of joints' properties based on

Janco et al. [18]. The base material was neither thermally affected nor mechanically deformed. It exhibited unaltered distribution in the grains and reinforcements.

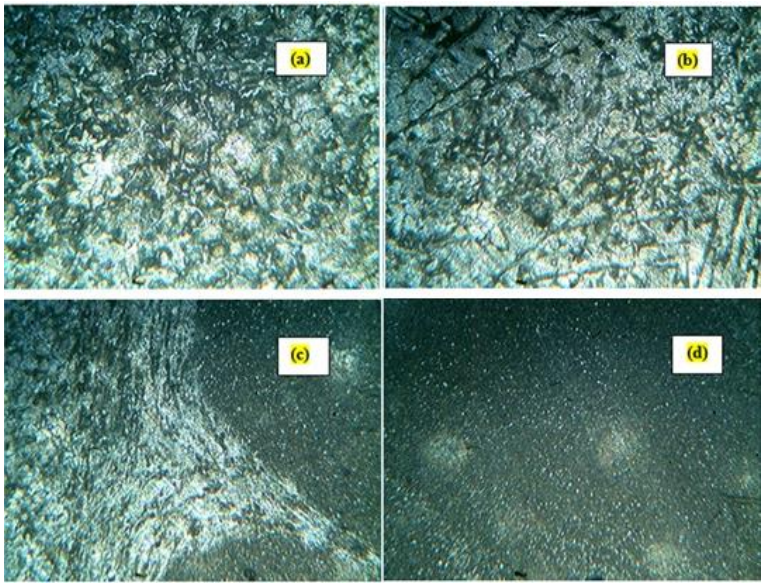

Fig. 6 Optical Microstructure of 3% nAl_2O_3 reinforced Al-13%Si Composite (a) Base Material, (b) Heat Affected Zone, (c) Transition Zone, (d) Nugget Zone

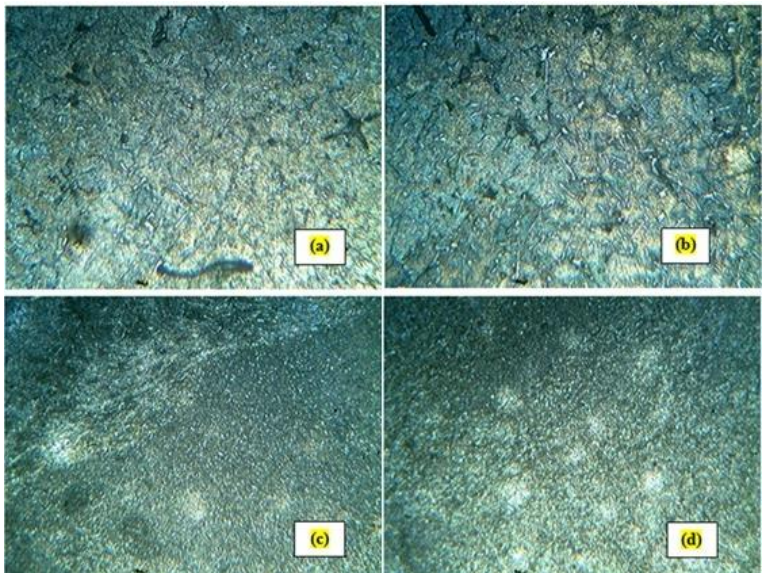

Fig. 7 Optical Microstructure of 6% nAl_2O_3 reinforced Al-13%Si Composite (a) Base Material, (b) Heat Affected Zone, (c) Transition Zone and (d) Nugget Zone

3.2 Mechanical properties

3.2.1 Tensile properties

The ultimate tensile strength of un-welded and welded composites of 0, 3 and 6% nAl_2O_3 is represented in Fig. 8. From this figure, it is clear that the tensile strength of the composite was increasing with increasing weight percentage of alumina nanoparticles. This increasing behaviour in the tensile strength was identical for both un-welded and welded samples. Reinforcement nanoparticles were envisioned to carry the load transferred by matrix of composites, so the composites with more nano-alumina reinforcements were able to withstand greater applied loads and hence possessed higher tensile strengths than that of composites having lower weight percentage of reinforcements. Also, it was envisaged that at the time of

solidification, nano-alumina reinforcements had provided more nucleation sites inside the melt which were envisioned to create a better homogeneous and fine grained morphological structure. Hard reinforcing particles were also contemplated to impede the excessive grain growth. Henceforth, the fine grains with higher reinforcing nanoparticles offered greater tensile strength than parent material or composites carrying lower content of nano-alumina reinforcements.

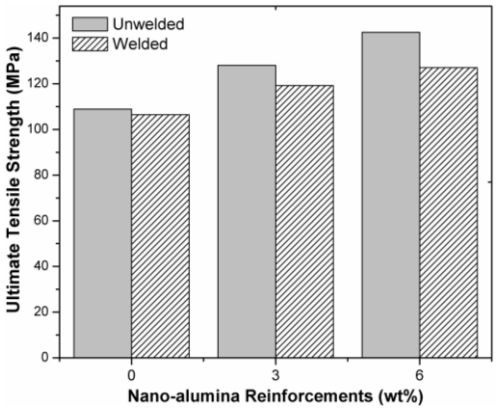

Fig. 8 Ultimate tensile strength of un-welded and welded composites

At the time of welding, due to tool stirring action, more homogeneous particle distribution was obtained and the size of the matrix grains were observed to be reduced within the weld zone. This tool action was believed to develop fine matrix grains with homogeneous distribution of reinforcing nanoparticles. This all may be the reason why FSW process has been expressed to possess better weld strength over other fusion welding processes.

3.2.2 Joint efficiency

Joint efficiency was calculated by taking the ratio of ultimate tensile strength of welded sample to that of an un-welded sample according to Equation 1. The joint efficiency was estimated to be reduced with increasing weight percentage of reinforcing nanoparticles as shown in Fig. 9. Increasing weight percentage of alumina nanoparticles increased the brittleness in composite and led to the reduction in ductility. So with increasing weight percentage of reinforcements, joint efficiency was decreased from 97 to 89%.

$$(\eta)\ \% = \frac{UTS of welded sample}{UTS of un-welded sample} \times 100 \qquad (1)$$

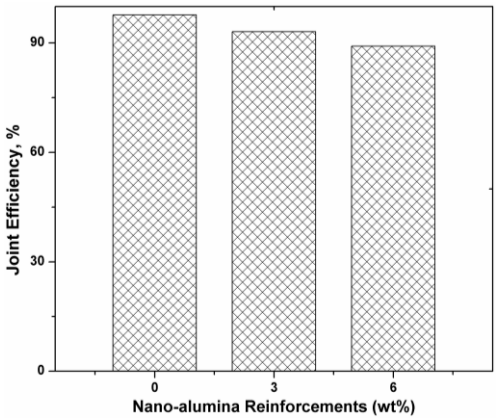

Fig. 9 Joint efficiency of a composite with different nano-alumina reinforcements

3.2.3 Hardness

The average value of hardness (BHN) of the four zones *i.e.* NZ, TMAZ, HAZ and unaffected BMZ of the friction stir welded 0, 3 and 6% nAl_2O_3 reinforced Al-13%Si was measured and shown in Fig.10. Silicon was contemplated to be responsible for enhancing the hardness of the parent alloy. Further increment in the hardness of the composite was noticed by adding hard nano-alumina reinforcements within the matrix. Hardness of the composite had a proportional relationship with the increasing weight percentage of reinforcements. Hard ceramic particles lowered the deformation and exhibited better hardness than parent alloy. Different zones of the FSW suffered differently, so hardness values were not observed uniform over all zones of the weld. Nugget zone was envisioned to suffer heavy dynamic recrystallization due to tool stirring action which was just below the tool probe. Clusters of reinforcement that were present in the parent composite were envisaged to be broken down by the tool action. Tool stirring actions also were responsible for the formation of fine grains within the matrix. Homogeneous distribution of reinforcing particles and recrystallized fine matrix grains were believed to be responsible for higher hardness of the nugget zone for all three types of composites. The TMAZ was observed to be mechanically deformed by the tool stirring action and therefore exhibited high hardness magnitudes. The TMAZ had somewhat lower hardness compared to the NZ because heat developed in the FSW had increased the grain size of the matrix to some extent. HAZ was the only zone that revealed coarse grains and exhibited the lowest hardness. The base material was relatively far enough from the tool to be affected by its action or the heat produced by it in FSW, therefore the original grain structures and particle distributions were not disturbed during FSW.

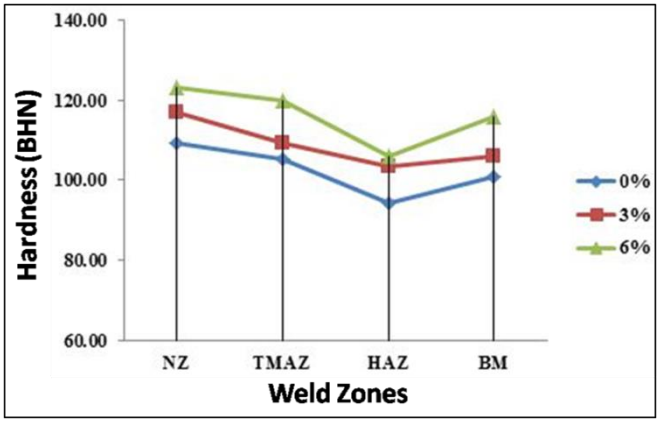

Fig. 10 Brinell hardness numbers related to various zones

3.3 Wear Properties

The dry sliding wear rate measurement of un-welded and welded specimen is shown in Fig. 11 (a) and (b) respectively. Dry sliding wear of material had an increasing behavior with increasing load. With increasing weight percentage of alumina reinforcement within the composites, the hardness was also observed to increase greatly, which is why the composite with higher magnitudes of reinforcement exhibited less wear as compared to lower ones. At the time of sliding, hard alumina nanoparticles offered greater wear resistance and protected the matrix against wear to a greater extent. Welded joints exhibited higher hardness owing to homogeneous distribution of alumina nanoparticles as compared to the parent composite; therefore, the dry sliding wear process was reduced in the welded specimens. It was also observed that during the starting period of the sliding test, a maximum wear rate was produced in all samples and after obtaining a certain temperature, the wear rate was reduced which may

be attributed to the formation of a protective oxide layer by the aluminium matrix. Hard alumina nanoparticles played a significant role in protecting the aluminium-silicon matrix from early wear against the hard surface of the sliding steel disc.

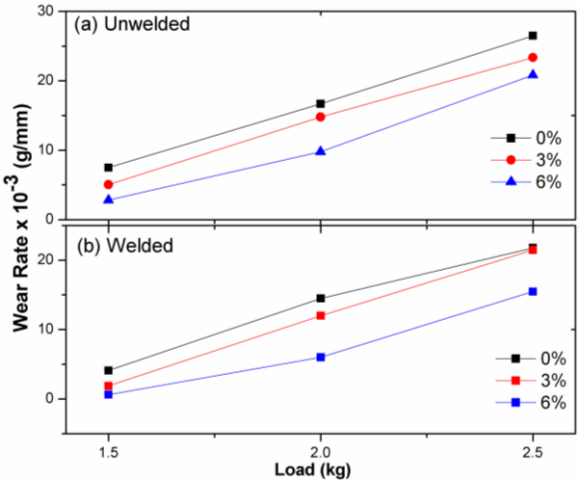

Fig. 11 Sliding wear rate of (a) un-welded, and (b) welded composites

4 Conclusion

- Mild steel tapered tool of specified geometry proved to be an appropriate material and geometry for FSW for Al-13%Si composites of different nAl_2O_3 reinforcements.
- The FSW parameters (tool traverse speed of 20 mm/min and rotational speed of 2000 rpm) produced good welded joints of 6mm thick plates made of these composites.
- Microstructure was observed to change thoroughly after FSW. Most refined grains with homogeneous distribution of particles had been illustrated in the nugget zone. TMAZ had totally different microstructure with rotating grains. There was no significant difference between the microstructure of HAZ and BMZ.
- The tensile strength was found to be increased with increasing weight percentage of nAl_2O_3 reinforcements. Friction stir welded samples exhibited lesser tensile strength as compared to un-welded samples.
- Joint efficiency of FSW samples was found to vary from 89-97%. Highest joint efficiency of 97% was exhibited in pure Al-13%Si alloy with the lowest of 89% observed within the composite of 6% nAl_2O_3 reinforcements. Joint efficiency was found to decrease with increasing weight percentage of nano-alumina reinforcements.
- NZ of welded samples exhibited the highest hardness among all four zones in all three types of composites. Hardness had a tendency to increase with increasing weight percentage of reinforcements. HAZ had lowest hardness due to presence of coarse grains. Maximum hardness of 123.18 BHN was shown in the NZ of 6% nAl_2O_3 reinforced composite. Minimum hardness of 94.23 BHN occurred in the HAZ of pure alloy. Silicon content and ceramic nanoparticles attributed for high hardness magnitude of these materials.
- Sliding wear had shown a decreasing trend with increasing hardness and reinforcement content. FSW samples had less wear as compared to un-welded samples. Homogeneous distribution of alumina nanoparticles and finer grains after FSW had resulted in less wear than in the BMZ. Wear rate was noted to be maximum for pure alloy and minimum for 6% reinforced composite. Harder nano-alumina particles were envisioned to protect the soft Al-13%Si matrix from wear. High silicon content was also assumed to play an important role in improving the wear resistance property of pure alloy and their nano-alumina composites.

ACKNOWLEDGEMENT

The authors gratefully acknowledge Technical Education Quality Improvement Programme (TEQIP) of the college to grant M. Tech. fellowship to Ms. Komal Rani and also financial support for testing and measurements.

REFERENCES

[1] W. Thomas, E. Nicholas, J. Needham, M. Murch, P. Temple-Smith, C. Dawes. Friction-stir butt welding, International patent application no. PCT/GB92/02203, **1991**.

[2] W. M. Thomas, E. D. Nicholas. Friction stir welding for the transportation industries, *Materials and Design*, **1997** (18), 269 - 273.

[3] S.W. Kallee, J. Davenport, E. D. Nicholas. Railway manufacturers implement friction stir welding, *Welding Journal*, **2002** (81), 47 - 50.

[4] M. R. Johnsen. Friction stir welding takes off at Boeing, *Welding Journal*, **1999** (78), 35 - 39.

[5] L. Ceschini, I. Boromei, G. Minak, A. Morri, F. Tarterini. Effect of friction stir welding on microstructure, tensile and fatigue properties of the AA7005/10vol.% Al_2O_{3p} composite, *Composites Science and Technology*, **2007** (67), 605 - 615.

[6] H. Uzun. Friction stir welding of SiC particulate reinforced AA2124 Al alloy matrix composite, *Materials and Design*, **2007** (28), 1440 - 1446.

[7] A. H. N. Byung-Wook, C. H. O. I. Don-Hyun, K. I. M. Yong-Hwan, U.N.G. Seung-Booj. Fabrication of SiCp/AA5083 composite via friction stir welding, *Transactions of Nonferrous Metals Society of China*, **2012** (22), 634 - 638.

[8] X.-G. CHen, M. D. Silva, P. Gougeon, L. ST-Georges. Microstructure and mechanical properties of friction stir welded AA6063–B_4C metal matrix composites, *Materials Science and Engineering: A*, **2009** (518), 174 - 184.

[9] S. J. Vijay, N. Murugan. Influence of tool pin profile on the metallurgical and mechanical properties of friction stir welded Al–10wt.% TiB_2 metal matrix composite, *Materials and Design*, **2010** (31), 3585 - 3589.

[10] H. Nami, H. Adgi, M. Sharifitabar, H. Shamabadi. Microstructure and mechanical properties of friction stir welded Al/Mg_2Si metal matrix cast composite. *Materials and Design*, **2011** (32), 976 - 983.

[11] S. Gopalakrishnan, N. Murugan. Prediction of tensile strength of friction stir welded aluminium matrix TiCp particulate reinforced composite, *Materials and Design*, **2011** (32), 462 - 467.

[12] I. Dinaharan, N. Murugan. Effect of friction stir welding on microstructure, mechanical and wear properties of AA6061/ZrB_2 in situ cast composites, *Materials Science and Engineering: A*, **2012** (543), 257 - 266.

[13] A. Vieirae, M. Ferrante. Prediction of rheological behavior and segregation susceptibility of semi-solid aluminium–silicon alloys by a simple back extrusion test, *Acta Materialia*, **2005** (53), 5379 - 5386.

[14] M. O. Shabani, A. Mazahery. Application of finite element method for simulation of mechanical properties in A356 alloy, *Int J Appl Math Mech*, **2011** (7), 89 - 97.

[15] H. Ye. An overview of the development of Al-Si-alloy based material for engine applications, *Journal of Materials Engineering and Performance*, **2003** (12), 288 - 297.

[16] S. Yigezub, D. Venkateswarlu, M. M. Mahapatra, P. K. Jha, N. R. Mandal. On friction stir butt welding of Al+12Si/10wt% TiC in situ composite, *Materials and Design*, **2014** (54), 1019 - 1027.

[17] A. Handa, V. Chawla. Experimental evaluation of mechanical properties of friction welded dissimilar steels under varying axial pressures, *Journal of Mechanical Engineering - Strojnícky časopis*, **2016** (66), No. 1, 27 - 36.

[18] R. Jančo, L. Écsi, P. Élesztős. FSW numerical simulation of aluminium plates by Sysweld - Part I, *Journal of Mechanical Engineering - Strojnícky časopis*, **2016** (66), No. 1, 47 - 52.